AIMS Energy, 10(4): 943–971.
DOI: 10.3934/energy.2022043
Received: 06 June 2022
Revised: 24 July 2022
Accepted: 29 July 2022
Published: 11 August 2022

http://www.aimspress.com/journal/energy

Research article

Multi-objective real-time integrated solar-wind-thermal power dispatch by using meta-heuristic technique

Sunimerjit Kaur[1,*], Yadwinder Singh Brar[2] and Jaspreet Singh Dhillon[3]

[1] Research Scholar, I.K. Gujral Punjab Technical University, Kapurthala 144603, Punjab, India
[2] Electrical Engineering Department, I.K. Gujral Punjab Technical University, Kapurthala 144603, Punjab, India
[3] Electrical and Instrumentation Engineering Department, Sant Longowal Institute of Engineering and Technology, Sangrur 148106, Punjab, India

* **Correspondence:** Email: sunimerriar@yahoo.co.in; Tel: +91 9855153770.

Abstract: The elevated demand for electrical power, expeditious expenditure of fossil fuels, and degradation of the environment because of power generation have renewed attentiveness to renewable energy resources (RER). The rapid augmentation of RER increases the convolutions in leveling the demand and generation of electrical power. In this paper, an elaborated α-constrained simplex method (ACSM) is recommended for multi-objective power dispatch problems. This methodology is devised after synthesizing the non-linear simplex method (SM) with the α-constrained method (ACM) and the evolutionary method (EM). ACSM can transfigure an optimization technique for the constrained problems by reinstating standard juxtapositions with α-level collations. The insertion of mutations and multi-simplexes can explore the periphery of the workable zone. It can also manage the fastness of convergence and therefore, the high precision solution can be obtained. A real-time multi-objective coordinated solar-wind-thermal power scheduling problem is framed. Two conflicting objectives (operating cost and emission) are satisfied. The case studies are carried out for Muppandal (Tamil Nadu), Jaisalmer (Rajasthan), and Okha (Gujarat), India. The annual solar and wind data are analyzed by using Normal Distribution and Weibull Distribution Density Factor, respectively. The presented technique is inspected on numerous archetype functions and systems. The results depict the prevalence of ACSM over particle swarm optimization (PSO), simplex method with mutations (SMM), SM, and EM.

Keywords: α-constrained simplex method; α-level comparisons; multi-simplexes; mutations;

normal distribution; weibull distribution density factor; fuzzy cardinal priority ranking

1. Introduction

Since the industrial uprising, the worldwide energy recoupment has been governed fundamentally by fossil fuels. This has crucial implications for the atmosphere. The expanded employment of RER can assist in the de-carbonization of the energy system in the future. This clean energy can help in dropping the inimical fossil fuel use and energy imports. Hence, it can portray an essential role in garnering the environment green and creating economic evolution.

With the expansion in the share of renewable energy associated with the power grid, the effectual collaboration of the function of different energy sources has emerged as a fresh challenge to the power system scheduling. The integrated operation of the RER-based power generation system may enhance the conflicts between electrical power generation and varying power outputs.

India is a country of geographical diversities. It has a large number of treasures of RER due to its magnificent topographical location. Its huge 'Thar Desert' of Rajasthan has high wind speeds and intense solar radiation. Its vast coasts are a great source of wind, solar, and tidal energies. It has sky-high 'Himalayan Mountain Ranges', which are the origin of thousands of water bodies and forests. Its large plains and plateaus have solar and wind energies, in abundance. To meet the power need and to turn down the role of fossil fuels in the power generation system, a large number of RER-based systems have already been implanted, in the country. Up to December 2019, the total RER-based instated capacity of India was 84 GW, with a set target of inducting 175 GW, by 2022 [1]. Therefore, the deployment of many more RER-based power generating systems is required, so that the rule of fossil fuels can be overthrown and quality power can be delivered to every needy, without much disturbing nature.

In the past, Liaquat et al. [2] have proposed multi-update position criteria for enhancing the investigation characteristics of the traditional firely technique while incorporating the effect of the globally best result on the fluctuation of the fireflies in the exploration zone of the objective function. They have put in the dynamic search space squeezing to compress the fireflies movement inside the definite boundaries to circumvent their oscillatory movement obtained while getting on for the global best solution by finding out the best trajectory for one and all fireflies. Rahimi and co-researchers [3] have elaborated a stochastic thermal and electric load scheduling problem considering the security constraints and also uncertainties of loads, RERs (wind and solar), and market price. They have used a scenario reduction approach to model all uncertain parameters. Naverson et al. [4] have adopted the continuous-time framework to design flexible hydropower sources negotiating with thermal generators (slow-ramping) to minimize the operation cost of the system. They have demonstrated their study through a small-scale case study in which a hydropower plant is connected to a thermal power plant with a manageable high voltage direct current cable.

Narang et al. [5] have applied the predator-prey optimization method for power scheduling of variable/fixed-head hydrothermal system. Predator assists to sustain heterogeneity in the swarm and also avert ill-timed convergence to the localized sub-optimal. They have used the variable elimination technique to control the equality constraint by abolishing variable exactness. Researchers in [6] have employed an adaptive predator-prey optimization to evaluate thermal power scheduling problems in a multi-objective framework. They have maintained the velocity of prey within limits by

acknowledging the supplementary and obstruction features.

Mondal and co-workers [7] have solved the economic load dispatch problem by considering both wind turbines and thermal generators to minimize fuel cost and NO_x emission by using Gravitational Search Algorithm. They have also investigated the influence of the wind system on NO_x emission. Ansari et al. [8] and Das et al. [9] have used the point estimate method to flourish the unreliability of wind and solar power systems. Das and co-workers have calculated the power generation cost with the crow search algorithm. Dasgupta and co-researchers [10] have employed the sine-cosine algorithm to minimize the cost of generation and emission pollutants. The parameters of the optimization technique have been used to balance the exploitation and exploration conditions to explore the optimal global solutions. Zhang et al. [11] have presented an enhanced borg (EBorg) algorithm to optimize a short-term dual-objective co-scheduling problem of a hydro-thermal-wind system. The EBorg framework has been comprised of ε dominance-based archive, crowding distance and pareto-dominance-based population upgrading mechanism, and auto-adaptive multi-operator reunification. They have worked on two objectives-generation cost and emission pollutants.

Reddy et al. [12] have presented an optimal power dispatch problem, considering an auction market with multi-mode, and solved it by using the genetic algorithm. They have maximized the total benefit of the participants at all nodes of the system. Ready has focused on the congestion management of an optimal power flow in the deregulated electricity market by using the multiobjective grenade explosion technique [13]. He has proposed a power flow problem in a multiobjective framework and optimized it by PSO. He has used fuzzy satisfying maximization for decision-making [14]. Salkuti has worked on a novel power scheduling of a hybrid system (wind, solar, and thermal generators) considering risk level and operating cost by using a non-dominated sorting genetic algorithm-II. He has optimized the real-time day-ahead divergence costs of the system [15]. He has considered an economic environmental dispatch problem having nonlinear features (valve point loading, ramp rate, prohibited operating zone effects, etc.) of thermal generators and optimized it with PSO [16]. He has presented an optimal feeder reconfiguration/network reconfiguration approach for minimizing operating cost and power losses of the system by using the crow search algorithm [17].

Zhang et al. [18] have developed a robust collaborative consensus algorithm for a dispersed economic dispatch having a practical communication network. The network has consisted of switching topology, noise, and transmission delay. Researchers in [19] have proposed the decentralized collaborative control structure of an independent virtual generation tribe (VGT) for a smart grid by using a VGT-based collaborative consensus algorithm (CCA) and a VGT-based robust CCA. Zhang et al. [20] have worked on a new cyber-physical-social system with parallel learning for distributed energy management of a microgrid. They have used the correlated equilibrium-based general sum game and the novel adaptive consensus algorithms for their work. Tan and co-workers [21] have presented a new fast learning optimizer for optimal energy management. Real-time non-convex energy management has been divided into two-layer optimization to reduce difficulties during optimization.

Biswas et al. [22] have employed success history-based adaptation method of differential evolution algorithm to solve optimal power flow incorporating uncertainty of wind and solar system with traditional thermal power generation system. They have employed lognormal probability distribution function and Weibull Distribution Functions for predicting solar and wind output power,

respectively. Das and co-researchers [23] have evaluated a hydrothermal scheduling problem deploying quasi-reflected symbiotic organisms search. This algorithm has been comprised of symbiotic organisms search to refine the execution of the prescribed technique.

He et al. [24] have used an upgraded combined binary and real number differential evolution technique based upon SHADE to present a model of coordinated power generation scheduling of hydro-thermal-wind system including spinning reserve. They have demonstrated the proposed model with an example and case study. Researchers in [25] have solved a multi-objective economic load dispatch problem with emended salp swarm algorithm. This algorithm includes the solitary and colonial phases of the reproduction cycle of life of salp. They have handled the equality constrained and prescribed functioning zone constraints.

Li et al. [26] have taken a large-scale hydro-wind-solar field in southwestern China to design an optimal power generation scheduling problem. They have maximized the total generated power and the minimum monthly collected output for the entire scheduling interim and minimized the environmental over & short discharge. Panda and Tripathy [27] have employed a new evolutionary hybrid algorithm for environmental optimal power flow problems including wind and thermal power generation systems. They have considered operational cost, emission cost, real power loss, and installation cost of FACTS devices to maintain a stable voltage.

Takahama and Sakai [28] have worked on the α-constrained simplex method (ACSM), to solve the constrained optimization problem of the real world. They have instated three modifications in the nonlinear simplex search method to obtain the borderline of the feasible zone, moderate the convergence speed, increase the accuracy, and enhance the overall efficiency of the system. Brar et al. [29] have suggested multi-objective fuzzy satisfying power generation scheduling by using simplex weightage pattern search. They have minimized four contradictory constraints and obtained real and reactive line flows by using generalized Z-bus distribution factors.

In this paper, a futuristic practice described as ACSM is executed to resolve a multi-objective real-time coordinated solar-wind-thermal power scheduling problem. It is a reconditioned unification of the SM introduced by Nelder and Mead. It is an improved conversion technique for constrained optimization. In this method, the non-linear simplex method is perceived as an evolutionary method in which a specific choice, substitution approach, and exceptional variation operator are employed to get high convergence speed, accuracy, and efficiency. It has been invented after hybridizing an established SM with certain other procedures (like-EM, α-constrained method, etc.). To frame this optimization method, three changes in the ordinary SM are executed: (i) α-level comparisons, (ii) the worst point's mutation, and (iii) use of multi-simplexes. In this study, three places from different parts of India are sorted out, where a coordinated solar-wind-thermal power system can operate efficiently. These marked out places are Muppandal (Tamil Nadu), Jaisalmer (Rajasthan), and Okha (Gujarat). A multi-objective coordinated solar-wind-thermal scheduling problem is formulated and optimized for the contemplated sites for two test systems, by using ACSM. To reflect the ascendancy of the suggested operating procedure, the outturns are differentiated with PSO, SMM, SM, and EM.

2. Optimal problem formulation

In the real world, the coordinated multi-objective optimization problems (CMOP) prerequisite the optimization of many contradictory constraints, concurrently. In this paper, two objectives of thermal

and RER systems are discerned. These objectives are total functioning cost and emission (NO_x, SO_2, & CO_2). Therefore, the CMOP is formulated as the minimization of two objectives subject to many equality and inequality constraints. All the objectives are evaluated discretely and then they are solved concomitantly using multi-objective configuration. Two objectives of interest (cost and emission) are of conflicting nature, especially in the case of thermal power generation system. An optimal solution to one can be attained at the cost of the other. Therefore, they are solved simultaneously to achieve the best compromise solution. These objectives can be stated as:

2.1. Optimal economy dispatch

The operating cost of a coordinated solar-wind-thermal power generating system depends upon the cost of fossil fuel and the functioning cost including the uncertainty cost of an RER-based power system. This objective can be conceived as the minimization of the total functioning cost of the system. The economy objective of the contemplated system can be examined as [30–34]:

$$F_1 = \sum_{i=1}^{Tg}(a_{Ti}Tp_i^2 + b_{Ti}Tp_i + c_{Ti}) + \sum_{j=1}^{Wg} Y_{wj} + \sum_{Q=1}^{Sg} Y_{SQ} \quad \text{(Rs/h)} \tag{1}$$

where Tg, Wg, and Sg are the number of thermal generators, wind generators, and solar units, respectively. Tp_i is the power output of the i^{th} thermal generator in MW. a_{Ti}, b_{Ti} and c_{Ti} are the cost coefficients of the i^{th} thermal generator. Y_{wj} is the wind power cost of the j^{th} wind generator. Y_{sQ} is the solar power cost of the Q^{th} solar unit.

2.2. Environmental objectives

Contrasting with RER-based plants the substantial environmental pollution is originated from the thermal power generation system, which is comprised mostly of nitrogen oxides (NO_x), sulfur dioxide (SO_2), and carbon dioxide (CO_2). In this paper, NO_x, SO_2, & CO_2 are specified as the emission determining index and treated as a single objective instead of three objectives. The economy and emission functions can be directly associated through the persistent factor known as emission rate per Mkcal for the defined grade and categorization of fossil fuel. The total thermal emission content is taken as the quadratic functions of thermal power output and can be expressed as [30–34]:

$$F_2 = \sum_{i=1}^{Tg}(d_{Xi}Tp_i^2 + e_{Xi}Tp_i + f_{Xi}) \,(\text{kg/h}) \tag{2}$$

where d_{Xi}, e_{Xi} & f_{Xi} are the emission coefficients of the i^{th} thermal generator and X is the emission (NO_x, SO_2, & CO_2).

2.3. Economic-environmental optimization problem

The goal of the multi-objective coordinated optimization problem for solar-wind-thermal power system is the acquisition of the optimal power dispatch by effectuating the minimization of incongruous objectives, simultaneously. The multi-objective power scheduling problem can be stated as [30–34]:

Minimize $[F_1, F_2]^T$
Subject to:
i. The equality constraint:

The total generated power of the solar-wind-thermal system must be equal to the addition of power demand and transmission losses. Therefore, the load demand equality constraint of the developed problem can be defined as [30–33]:

$$\sum_{i=1}^{Tg} Tp_i + \sum_{j=1}^{Wg} Wp_j + \sum_{q=1}^{Sg} Sp_q = P_D + P_{Loss} \quad (3)$$

where Wp_j is the scheduled power of the j^{th} wind generator in MW. Sp_Q is the scheduled power of the Q^{th} solar unit in MW. P_D is the system power demand in MW. P_{Loss} is the total system transmission losses in MW.
ii. Power generation limits of generating units:

The decision variables of thermal, wind, and solar systems (Tp_i, Wp_j, & Sp_Q) must lie between the power generation limits of the respective generating unit. The lower and upper generation limits enforced on thermal, wind, and solar power generating units are [30–33]:

$$Tp_{imin} \le Tp_i \le Tp_{imax} \ (i = 1,2, \dots, Tg) \quad (4)$$

$$0 \le Wp_j \le Wpr_j \ (j = 1,2, \dots, Wg) \quad (5)$$

$$0 \le Sp_Q \le Spr_Q \ (Q = 1,2, \dots, Sg) \quad (6)$$

where Tp_{imin} and Tp_{imax} are lower and upper limits of the power output of the i^{th} thermal generator in MW, respectively. Wpr_j is the rated power output of the j^{th} wind generator and Spr_Q is the rated power output of the Q^{th} solar unit in MW.

2.4. Model of uncertainty of wind generators

Electrical power generation has arisen as the principal implementation of wind energy, globally. This energy renders an accepted contemporary power generation source and a vital participant in the world's energy trade. Wind power generation exceedingly depends upon wind speeds. To procure the precise solution of wind power dispatch prognostication of wind power is decisive. In this paper, the Weibull Distribution Density Factor is used to examine irregular wind data. The wind speed variations are demonstrated by using the Probability Density Function (PDF) and it can be evaluated as [32–36]:

$$F_{PDF} = \left(\frac{k}{c}\right)\left(\frac{v}{c}\right)^{k-1} exp\left[-\left(\frac{v}{c}\right)^{k}\right], (0 \le v \le \infty) \quad (7)$$

where is the annual average wind speed in m/sec. *k* is the shape factor. *c* is the scale factor in m/sec.

The shape factor is a parameter that displays the span of allocation of wind speeds. It can be obtained as [32,34]:

$$k = \left(\frac{\sigma}{v_m}\right)^{-1.086} \tag{8}$$

where v_m and σ are the mean wind speed and the mode wind speed, in m/sec, respectively.

The scale factor displays the capability of the wind power of that location. It can be defined as [32,34]:

$$c = \frac{v_m}{\Gamma(1+\frac{1}{k})} \tag{9}$$

The Gamma Function has frequently applied extension of the factorial functions to the complex numbers and can be observed as [32,34]:

$$\Gamma(x) = \int_0^{\infty} e^{-t}\, t^{x-1}\, dt \tag{10}$$

Wind energy approximation is decisive to guarantee grid regulation and optimal wind power dispatch. Wind velocity distribution for a specific wind power zone can be designed by using probability distribution functions (PDF). The PDF of wind power can be expressed as [32,34]:

$$f(Wavj) = \begin{cases} \left(\frac{k\, I_j v_{inj}}{c}\right)\left(\frac{(1+\rho_j I_j)v_{inj}}{c}\right)^{k-1} exp\left[-\left(\frac{(1+\rho_j I_j)v_{inj}}{c}\right)^{k}\right]; & for\ 0 < v_{op} < v_{Rj} \\ 1 - \exp\left[-\left(\frac{v_{Rj}}{c}\right)^{k}\right] + exp\left[-\left(\frac{v_{0j}}{c}\right)^{k}\right] \quad ; & for\ v_{op} = 0 \\ \exp\left[-\left(\frac{v_{Rj}}{c}\right)^{k}\right] - exp\left[-\left(\frac{v_{0j}}{c}\right)^{k}\right] \quad ; & for\ v_{op} = v_{Rj} \end{cases} \tag{11}$$

where v_{inj}, v_{Rj}, & v_{oj} are the cut-in speed, the rated speed, and the cut-out speed of the j^{th} wind generator in m/sec, respectively. v_{op} is the operating wind speed in m/sec.

$$\rho_j = \frac{v_{op}}{v_{Rj}} \tag{12}$$

$$I_j = \frac{(v_{Rj} - v_{inj})}{v_{inj}} \tag{13}$$

The available wind power at a particular location depends upon the specifications of the j^{th} wind generator and operating wind speeds during the considered period. The available wind power for the j^{th} wind generator, at different wind velocities, can be calculated as [32–35]:

$$Wavj = \begin{cases} 0 & ; for\ v_{op} < v_{inj} and v_{op} > v_{oj} \\ \frac{Wpr_j(v_{op} - v_{inj})}{(v_{Rj} - v_{inj})} & ; for\ v_{inj} < v_{op} < v_{Rj} \\ Wpr_j & ; for\ v_{Rj} \le v_{op} \le v_{oj} \end{cases} \tag{14}$$

Electrical power systems which assimilate RER have to deal with unreliability about the accessibility of load or injected power. This causes the consideration of uncertainty costs in the representation of stochastic economic dispatch. The observation of these costs is vital for the accepted management of RER and the proper issuance of the available energy amount for the power

system. The actual cost of wind power is often found more than its anticipated cost. The direct cost function of the j^{th} wind generator can be evaluated as [32,34]:

$$y_{dwj} = y_{w1j} Wp_j \tag{15}$$

where y_{w1j} is the direct cost coefficient of the j^{th} wind generator.

When the actual wind power is found less than the planned wind power, the operator has to a pay penalty cost, which is called the overestimation cost. The overestimation cost function of the j^{th} wind generator is determined as [32,34]:

$$y_{owj} = y_{w2j} \int_0^{Wpj} (Wp_j - Wavj)\, f(Wavj) d(Wavj) \tag{16}$$

where y_{w2j} is the overestimation cost coefficient of the j^{th} wind generator.

On the other hand, underestimation cost is fine for not utilizing the available wind power for the certain duration. The underestimation cost function of the j^{th} wind generator can be obtained as [32,34]:

$$y_{uwj} = y_{w3j} \int_{Wpj}^{Wprj} (W_{avj} - W_{pj})\, f(W_{avj}) d(W_{avj}) \tag{17}$$

where y_{w3j} is the underestimation cost coefficient of the j^{th} wind generator.

The total operating wind power cost of the j^{th} wind generator is equal to the sum of the direct cost, the overestimation cost, and the underestimation cost, for a specific time. The total operating cost function of the j^{th} wind generator can be stated as [32–34]:

$$Y_{wj} = y_{dwj} + y_{owj} + y_{uwj} \tag{18}$$

2.5. Model of uncertainty of solar units (PV)

Solar energy can be pivotal to the clean energy future. The sun daily radiates far more energy than the power requirements of all the human beings on earth. Solar radiations vary with the topography and climate of a certain area. In this paper, to analyze the irregular solar data, normal distribution is utilized. The Probability Density Function (PDF) of solar irradiance can be calculated as [31,34]:

$$fs(I_t) = \frac{e^{\frac{-(I_t - M)^2}{2D^2}}}{D\sqrt{2\pi}} \tag{19}$$

where I_t is the solar irradiance at a given time, M is the mean of solar irradiance over the year, and D is the standard deviation of solar irradiance, in kWh/m^2/day.

The available power of the Q^{th} solar unit can be evaluated as [31,33,34]:

$$\mathrm{S_{avQ}} = \mathrm{Spr_Q} \frac{(1 + \mathrm{k_a}(\mathrm{T_o} - \mathrm{T_{rQ}}))\mathrm{I_r}}{\mathrm{I_m}} \tag{20}$$

where T_o is the operating temperature and T_{rQ} is the reference temperature of the Q^{th} solar unit, in ºC. k_a is the temperature coefficient in /ºC. I_m is the maximum value of solar radiation incident under standard conditions in kWh/m^2/day.

Solar radiation is a broad expression for the electromagnetic radiation discharged by the sun. These can be seized and converted into useful formations of energy, such as electricity and heat, employing different technologies. The solar radiations incident on an inclined plane is expressed as [31,33,34,37]:

$$I_r = \frac{I_t[\cos(\emptyset - A)\cos\delta\ \cos\omega + \sin(\emptyset - A)\sin\delta]}{(\cos\delta\cos\omega\cos\emptyset + \sin\emptyset\cos\delta)} \tag{21}$$

where $\emptyset$ is geographical latitude, A is the angle of the tilt of the solar collector, δ is the sun's declination, and ω is the hour angle, in degrees. $A = \emptyset \pm 15°$

The declination angle of the sun varies seasonally because of the Earth's tilt on its rotation axis and its rotation around the sun. This angle would always be 0° if the Earth were not leaning on its rotation axis. As the Earth is sloped by 23.45° and the angle of declination depends upon this amount [37]. The angle of the sun's declination can be obtained as [31,33,34]:

$$\delta = 23.45° \sin\left(\frac{360(284 + d_n)}{365}\right) \tag{22}$$

where d_n is the number of the day of the year.

Similar to the wind power system, due to the unsure conduct of the sun, the forecasted solar power may not always be equal to the scheduled solar power. The operating cost of the solar power system also depends upon the direct cost and the uncertainty cost of the solar unit. The direct cost function of the Q^{th} solar unit can be determined as [31,34]:

$$y_{dsQ} = S_{1sQ} Sp_Q \tag{23}$$

where S_{1sQ} is the direct cost coefficient of the Q^{th} solar unit.

The penalization for deploying another energy resource or for not supplying energy is called overestimation cost as discussed in the wind system. The overestimation cost function of the Q^{th} solar power unit is given as [31,34]:

$$y_{osQ} = S_{2sQ}\left(Sp_Q - S_{avQ}\right) fs(I_t) \tag{24}$$

where S_{2sQ} is the overestimation cost coefficient of the Q^{th} solar unit.

The castigation for not utilizing all the available power or the underestimation cost function of the Q^{th} solar power unit can be obtained as [31,34]:

$$y_{usQ} = \left\{S_{3sQ}\left(S_{avQ} - Sp_Q\right)\right\} fs(I_t) \tag{25}$$

where S_{3sQ} is the underestimation cost coefficient of the Q^{th} solar unit.

The total operating cost of the Q^{th} solar unit can be evaluated as [31,34]:

$$Y_{SQ} = y_{dsQ} + y_{osQ} + y_{usQ} \tag{26}$$

2.6. Transmission losses

These losses directly rely upon the characteristics of the network and the operation mode. They are mostly caused by energy dissipation in the conductors, appliances used in transmission lines, etc. Regardless of how the electrical power system is modeled, these losses are unpreventable and must be fabricated before depiction can be evaluated. In this paper, the transmission losses of the coordinated solar-wind-thermal power system are obtained by making use of Kron's approximated loss formula through beta-coefficients and these can be expressed as [30–34]:

$$P_{TLoss} = \sum_{i=1}^{Tg}\left(\sum_{j=1}^{Tg} Tp_i B_{TiTj} Tp_j\right) \tag{27}$$

$$P_{WLoss} = \sum_{i=1}^{Wg}\left(\sum_{j=1}^{Wg} Wp_i B_{wiwj} Wp_j\right) \tag{28}$$

$$P_{SLoss} = \sum_{i=1}^{Sg}\left(\sum_{j=1}^{Sg} Sp_i B_{sisj} Sp_j\right) \tag{29}$$

where P_{TLoss}, P_{WLoss}, and P_{SLoss} are the transmission losses due to the thermal system, the wind system, and the solar system respectively, in MW.

Total transmission losses of the system can be evaluated as [31–34]:

$$P_{Loss} = P_{TLoss} + P_{WLoss} + P_{SLoss} \tag{30}$$

3. Solution Procedure

In this paper, ACSM is applied to optimize the proposed real-time constrained power scheduling problem. In this technique, SM is upgraded by inlaying α-level comparisons rather than ordinary comparisons, mutations of the worst points, and multi-simplexes as a substitute for a single simplex.

The α-level comparisons are used to transform algorithms for unconstrained optimization problems into algorithms for constrained optimization problems. By employing these comparisons, the search points are compared based on the pre-defined satisfaction level of their constraints. It means that the points are differentiated on the grounds of their constraint infringement.

The optimal solutions to the constrained problems are frequently found near the frontier of the feasible region. Therefore, to explore the points around the boundary of the feasible zone, the mutations to the worst points and multi-simplexes are adjoined, in the algorithm. It can also control the convergence speed.

3.1. Refinements to the nonlinear simplex method

The nonlinear simplex method is upgraded by performing the following alterations to enhance its efficacy [28]:

(i) α-level collations:

To transfigure a constrained optimization problem to an unconstrained optimization

problem, α-level comparisons can be applied in place of usual comparisons. Consider $f(z)$ is an objective function and $\mu(z)$ is its satisfaction level. The α-level comparisons are the order relation on $(f(z), \mu(z))$ set, in which the viability of z is more vital than minimizing $f(z)$. α-level collations between any two objective functions f_A & f_B having satisfaction levels μ_A & μ_B respectively and can be stated as follows:

$$(f_A, \mu_A) <_\alpha (f_B, \mu_B) <=> \begin{cases} f_A < f_B, \ ; if \mu_A, \mu_B \geq \alpha \\ f_A < f_B, \ ; if \mu_A = \mu_B \\ \mu_A > \mu_B \quad ; else \end{cases} \tag{31}$$

$$(f_A, \mu_A) \leq_\alpha (f_B, \mu_B) <=> \begin{cases} f_A \leq f_B, \ \ if \mu_A, \mu_B \geq \alpha \\ f_A \leq f_B, \ \ if \mu_A = \mu_B \\ \mu_A > \mu_B, \ \ else \end{cases} \tag{32}$$

The value of α lies between 0 and 1. The α level collations are analogous to the usual differentiations if the value of α is zero.

(ii) Incorporation of mutations:

In constrained optimization problems usually, the optimal solutions are found very close to the borderline of the feasible province. While solving these problems with the help of the nonlinear simplex method, when simplex reduces some search points encircling the boundary of the feasible zone are ignored, sporadically. Therefore, to evade such situations mutations are included because they are capable of producing optimal results surrounding the frontier of the feasible stretch of the surveyed points. The least desirable point is exchanged by mutations utilizing Eqs (46,47).

Mutations can also sway the consolidation speed of the algorithm. Therefore, the preferable value of the mutation rate should be picked out. High values of mutation rate gravitate towards a large number of calculations and therefore sometimes computation speed may decay.

(iii) Inclusion of multi-simplexes:

In the nonlinear simplex method, simplex may overlook affine autonomy occasionally and therefore this technique can't search for the optimal solutions. To handle such situations multi-simplexes are included. The affine autonomous simplexes can work for the optimal solutions, even when some simplexes mislay affine sovereignty. In a nonlinear simplex method, for the decision variable of n dimension, initially, $n+1$ points are searched, whereas to formulate multi-simplexes at least $n+2$ points are generated.

The count of explored points regulates the diversification of the investigation operation and also the simulation speed. If the number is very small but the convergence speed is lofty the surveyed points usually concur to a confined optimum. If the number is very large and the convergence speed is low, the explored points can't arrive at the global optimum.

3.2. Algorithm of ACSM

Consider $f(z^i)$ is an objective function, where z^i is an n-dimensional vector of decision variable such that $(i = 1,2, \ldots \ldots, N)$. The algorithm of ACSM can be stated as [28,33,34]:

(1) Put expansion factor $\gamma > 1$, contraction factor $b \in (0,1)$, mutation rate $P_M \in (0-1)$, tolerance limit Ɛ=0.001, algorithm parameters β=0.03, and T_α=50.

(2) Randomly generate the initial search points ($N\ (>n+1)$) in the extremities of the search zone. Scrutinize the i^{th} dimension arbitrarily and now either the upper limit or the lower limit is designated to z^i. The remaining variables are created inconstantly betwixt the upper limit and lower limit of each variable.

(3) Determine the feasible solution by employing the designed casual heuristic search approach. In this paper, two distinct search proceedings are executed auspiciously to attain the feasible solution that delivers the solar-wind-thermal power generations during appeasing the equality constraints (Eq (3)). One strategy is to encounter the accessible power demand constraint of the system over the inspected interim. The second maneuver is based upon the handling of the uncertainty of the RER system using Eq (7) to Eq (26).

(4) All the objectives and objective functions commensurate to inequality constraints of the solar-wind-thermal generation problem are collaborated to evaluate the amalgamated impact of all the objectives concurrently deploying their membership functions Eq (44). The maximum value of the clubbed membership function demonstrates the satisfaction level analogous to the non-inferior produce of the objective function Eq (45).

(5) Obtain z^l (the best point), z^h (the worst point), and z^s (next to the worst point), by using the following equations:

$$z^l = arg\,min_i\ f(z^i) \tag{33}$$

$$z^h = arg\,max_i\ f(z^i) \tag{34}$$

$$z^s = arg\,max_{i\neq h}\ f(z^i) \tag{35}$$

(6) Create the random number R and rationalize z^h as:

$$z^h = \begin{cases} z^l + R(z^h - z^l) & ;R \geq P_M \quad (36) \\ z^h - R(z^h - z^l) & ;\text{Else} \quad (37) \end{cases}$$

(7) Skip the worst point and form the initial simplex with $n+1$ points. Find the centroid of the simplex from the following equation:

$$z^0 = \frac{1}{n+1}\sum_{\substack{i=1 \\ i\neq h}}^{n+1} z^i \tag{38}$$

(8) The value of the α can be restrained as stated in Eq (39). The starting value of α is α_0 and it is found in the initial search. It is computed as the average of the best satisfaction level value and the mean of the total satisfaction level values. When the iteration number alters to t, the value of α is upgraded as the multiple of T_α. The value of α is disposed to 1 when the iteration number exceeds $\frac{T_{max}}{2}$. Its values lie between (0–1).

$$\alpha(t)=\begin{cases}\frac{1}{2}\left(best\left(\mu_d(z^i)\right)+\frac{1}{N}\sum_{i=1}^{N}\mu_d(z^i)\right) & ;t=0\\ (1-\beta)\alpha(t-1)+\beta & ;\ 0<t\le\frac{T_{max}}{2}\text{and}(t\ mod\ T_\alpha)=0\\ \alpha(t-1) & ;0<t\le\frac{T_{max}}{2}\text{and}(t\ mod\ T_\alpha)\neq 0\\ 1 & ;t>\frac{T_{max}}{2}\end{cases} \tag{39}$$

where t is the iteration number. T_{max} is the maximum number of iterations.

(9) Calculate the reflected point z^r by reflecting the best point about the centroid, with the support of the following equation:

$$z^r=(1+\alpha)z^0-\alpha z^h \tag{40}$$

(10) If z^r is superior to the best point, ie.$\left(f(z^r),\mu_d(z^r)\right)<_\alpha\left(f(z^l),\mu_d(z^l)\right)$, then go to step 11, else go to step 12.

(11) The expansion process takes place, in which with the help of reflection operation the simplex progresses towards the better zone of the search space. Determine the expansion point z^e as:

$$z^e=\gamma z^r+(1-\gamma)z^0 \tag{41}$$

If the expansion point is more reformed than the best point, i.e., $\left(f(z^e),\mu_d(z^e)\right)<_\alpha\left(f(z^l),\mu_d(z^l)\right)$, then z^h is reinstated by z^e, else z^h is replaced by z^r, and go back to step 4. Figure 1 represents the flowchart of ACSM.

(12) If the reflection operation drags the simplex towards the deplorable zone, i.e., the reflection point is finer than and equal to the next to the worst point of the simplex $\left(\left(f(z^r),\mu_d(z^r)\right)\le_\alpha\left(f(z^s),\mu_d(z^s)\right)\right)$, then displace z^h by z^r and go back to step 4, else go to step 13.

(13) If the worst point is less scholarly than the reflected point, i.e., $\left(f(z^r),\mu_d(z^r)\right)<_\alpha\left(f(z^h),\mu_d(z^h)\right)$, then z^h is replaced by z^r and go to step 4, else evaluate contraction process is supervened. The contraction point z^c can be calculated as:

$$z^c=bz^h+(1-b)z^0 \tag{42}$$

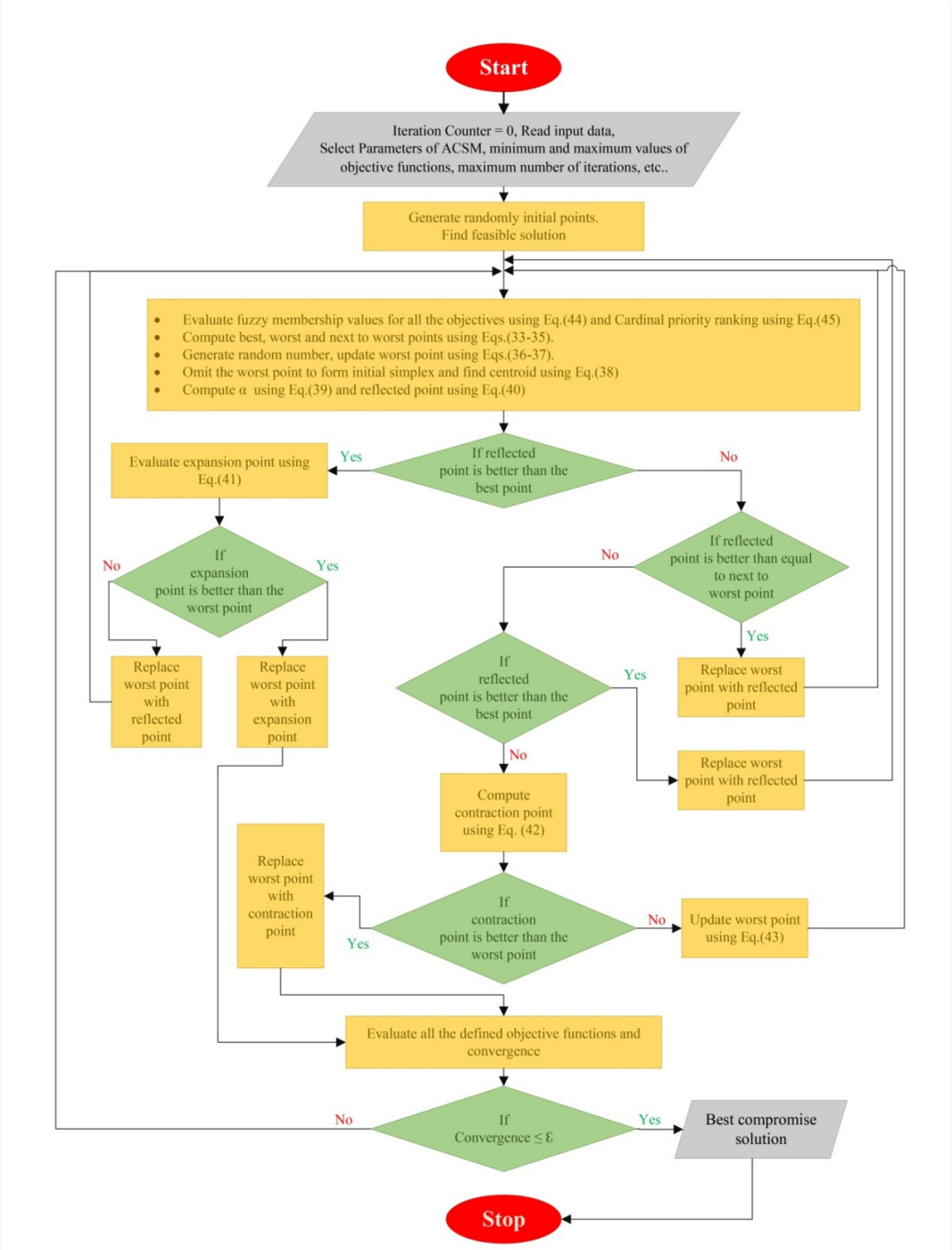

Figure 1. Flowchart of α-Constrained simplex method.

If $\left(f(z^c), \mu_d(z^c)\right) <_\alpha \left(f(z^h), \mu_d(z^h)\right)$, then z^h is replaced by z^c, else update z^h as:

$$z^h = bz^h + (1-b)z^l \tag{43}$$

and go back to step 4.

(14) Evaluate all the objective functions.

(15) Check the stopping criteria. If abs $(f^l - f^h) \leq \varepsilon$ then go to step 16, else go back to step 4.

(16) Stop.

The contraction factor controls the convergence speed of the computation process. If it is small the investigating process reaches its centroid very soon. If the convergence speed is high the search operation may omit the global optima and coincide with local optima. If the contraction factor is very large the processing speed turns out to be low therefore search may not attain global optima.

The feasible zone can be extended by moderating the value of α and the extended feasible zone can be brought down to the primal by increasing the value of α to 1, in a constrained SM. The value of β regulates the growing speed of α and the speed of bringing down the extended feasible zone. The value of α reaches 1 moderately if the value of β is less. Here, the possibility that the explored points approach to local optimum is less. If the value of β is very small the explored points must examine a large area, therefore efficacy reduces. If the extended zone happens to be large at the half iterations, the explored points might reach to feasible zone quickly therefore, it can omit the global optima [28].

3.3. Decision-making

The decision-making has an indefinite character and fuzzy targets for the objective functions. The goals comprise categories of alternatives whose limits are not distinctly defined. The fuzzy goals and fuzzy objectives can be defined accurately as fuzzy sets in the zone of substitutes. Here, a fuzzy decision can be observed as the junction of the specified targets and objectives. These fuzzy aims are adjusted by establishing their membership functions, whose values vary from 0–1. The value 0 of the membership function means irreconcilability and value 1 indicates complete complementarity. It can be defined as [30–34]:

$$\mu(\mathrm{F_i}) = \begin{cases} 1 & ; f_i \leq f_i^{min} \\ \frac{f_i^{max} - f_i}{f_i^{max} - f_i^{min}} & ; f_i^{min} < f_i < f_i^{max} \quad (i = 1,2,\ldots,M) \\ 0 & ; f_i \geq f_i^{max} \end{cases} \tag{44}$$

where f_i is the objective function. f_i^{max} and f_i^{min} are the maximum and minimum values of the objective function, respectively.

The Fuzzy Cardinal Priority Ranking (the membership function) of the non-dominated (pareto-optimal) solution to a fuzzy set can be stated as [30,33,34]:

$$\mu_d^K = \frac{\sum_{i=1}^{M} \mu(f_i^K)}{\sum_{k=1}^{K} \sum_{i=1}^{M} \mu(f_i^K)} \tag{45}$$

where K is the number of non-dominated solutions.

4. Case studies and results

The optimization problems of the electrical power systems (EPS) are very strenuous to solve because the EPSs are very sizeable, composite, structurally extensively distributed, and are impacted by several unpredicted circumstances. Real-time optimization techniques utilize the accessible computations in the optimization structure and are, thus, competent in conducting the appropriate self-optimizing regulation. In this paper, a real-time multi-objective coordinated solar-wind-thermal power scheduling problem is optimized for three different places in India, by using ACSM. The names of these places are:

1. Muppandal (Tamil Nadu)
2. Jaisalmer (Rajasthan)
3. Okha (Gujarat)

The same set of power generating units (PGU) and coefficients (cost and emissions) are used for all three places, to access the performance of PGU in the different geographical and environmental conditions. The functions of cost coefficients of the RER power system are also taken as the same for all three sites. This work is executed with the help of the FORTRAN-90 programming language using ACSM and results are collated with PSO, SMM, SM, and EM.

4.1. Geographical positions and renewable energy potentials of Muppandal, Jaisalmer, and Okha

India is the seventh-largest country in the world and it lies on the north of the equator between 8°4' north to 37°6' north latitude and 68°7' east to 97°25' east longitude [38]. It possesses large topographical and meteorological variations. Many parts of the country are rich in solar and wind energies. Muppandal, Jaisalmer, and Okha are among such places.

Muppandal is a village in the Kanyakumari district of Tamil Nadu state of India. It is situated at the southernmost point of India. It has India's largest wind farm, with a 1500 MW installed capacity [39,40]. Jaisalmer city of Rajasthan is placed in the northwestern region of India. It is a segment of the 'Great Indian Thar Desert'. India's second-largest wind farm of 1064 MW capacity, is installed here [41]. Okha is a famous town in the Dwarka district of Gujarat state. It is a port at the west-central tip of India. It has a high solar and wind energy prospect. The solar and wind parameters of these three sites are tabulated in Table 1.

Table 1. Solar and wind parameters of Muppandal, Jaisalmer, & Okha.

System variables	Muppandal	Jaisalmer	Okha
Geographical latitude-Ø (degrees)	8.15	26.95	22.469
Annual average solar irradiance (kWh/m^2/day)	5.68	5.79	5.86
Average solar irradiance of June (kWh/m^2/day)	5.48	5.47	4.74
Reference temperature (°C)	32	41	33
Mean wind speed (m/sec)	11.50	9.00	8.70
Mode speed (m/sec)	5.50	3.42	2.90

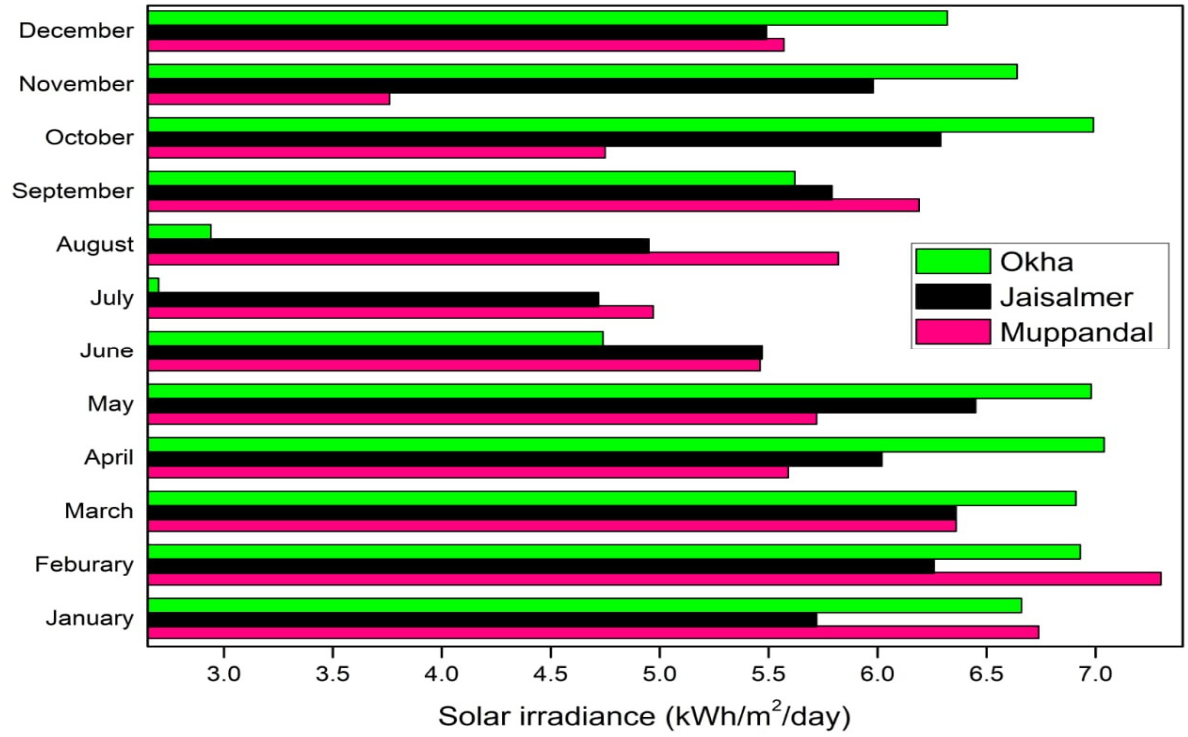

Figure 2. Variation of solar radiations in Muppandal, Jaisalmer, & Okha, over the year.

Every single locality on Earth acquires solar radiation at the minimum fragment of the year. The quantity of solar radiation that arrives at any one part on the surface of Earth differs according to geographic location, time of day, season, local weather, local landscape, etc. Due to the round shape of Earth, the sun hits the surface at dissimilar angles, varying from 0° to 90° [37]. When the rays of the sun are vertical the surface of Earth achieves all the possible energy. If the sun's rays are more tilted, they travel through the atmosphere for a longer period and therefore, become more diffused and scattered. Figure 2 displays the variation of solar radiation in three considered zones, over the year. It can be seen that all three locations have a high value of solar radiation (except in the monsoon season, from June to August). The maximum drops of radiation can be seen in Okha during this season. Therefore, it has the minimum value of available solar power, in this span of the year.

The mean and mode wind speeds of the year are nearly 11.50 m/sec, 9.0 m/sec & 8.70 m/sec, and 5.50 m/sec, 3.42 m/sec & 2.90 m/sec, respectively for Muppandal, Jaisalmer, and Okha.

4.2. Simulation and results

In fact, because of the intermittency of wind and solar radiation, generating extra power results in increasing output fluctuations. Therefore, in this paper, an integrated scheduling model of a territorial RER-based energy system combined with a conventional thermal power generation system is established to encounter the oscillating power requirements of consumers. The considered coordinated solar-wind-thermal power system contains six generating units (two thermal generators, two solar units, and two wind farms).

Table 2. The characteristic fuel and emission functions of two thermal generators.

Fuel cost (Rs/h) equations	NO_x emission (kg/h) equations
F_{11} = 0.001345 Tp_1^2 + 8.30154 Tp_1 + 274.2241	$F_{21} = 0.006732Tp_1^2 - 2.39928Tp_1 + 610.2535$
F_{12} = 0.005963 Tp_2^2 + 6.91559 Tp_2 + 202.0258	$F_{22} = 0.006181Tp_2^2 - 0.39077\ Tp_2 + 50.3808$
SO_2 emission (kg/h) equations	CO_2 emission (kg/h) equations
F_{31} = 0.000813 Tp_1^2 + 4.97641 Tp_1 + 165.3433	$F_{41} = 0.106409Tp_1^2 - 12.73642Tp_1 + 1819.625$
F_{32} = 0.003578 Tp_2^2 + 4.14938 Tp_2 + 121.2133	$F_{42} = 0.403144Tp_2^2 - 121.9812Tp_2 + 11381.07$

The fuel costs functions and the pollutant emission (NO_x, SO_2 & CO_2) functions of two thermal generators are given in Table 2. The fuel cost functions and pollutant emission functions are minimized over the set of permissible decision vector Tp_i. The minimum and maximum generation limits of each thermal generator are taken as 10 MW and 250 MW, respectively.

Table 3. Parameters of solar units (PV).

Solar system variables	Specifications
Hour angle (°)	−15
The angle of tilt of the solar collector (°)	20
Temperature coefficient (/°C)	$-4.7\ e^{-3}$
The capacity of each solar unit (MW)	30
Coefficient of direct cost (Rs/kWh)	4.50
Coefficient of underestimation cost (Rs/kWh)	17.280
Coefficient of overestimation cost (Rs/kWh)	12.280

The solar system parameters for the 15th day of June of each year are enlisted in Table 3 and wind system parameters are charted in Table 4. At 1 PM the value of the hour angle is found as −15°. The values of angle of tilt of solar collector and cost coefficients of solar & wind systems are contemplated as the same for the described sectors of India.

The fuel cost and the emissions (NO_x, SO_2 & CO_2) of the thermal generating system are obtained by using Eqs (1) and (2). The power balance Eq (3) is solved, subject to the equality constraint and power generation limits of thermal generators, wind generators, and solar units, using Eqs (4–6). The wind data is contemplated according to the Weibull distribution density function. The PDF of wind behavior is observed from Eq (7). The shape factor 'k' is evaluated from the mean and the mode wind speeds by using Eq (8), which is found as 2.229, 2.86 & 3.33 for Muppandal, Jaisalmer, and Okha, respectively. The scale factor 'c' is calculated from Eqs (9) and (10), by using the Gamma

Function. These values are obtained as 12.981 m/sec, 10.099 m/sec, and 9.695 m/sec for Muppandal, Jaisalmer, and Okha, respectively.

Table 4. Parameters of wind farms.

Wind system variables	Specifications
The capacity of each wind farm (MW)	30
Cut in velocity v_i (m/sec)	3.5
Cut out velocity v_o (m/sec)	25
Rated speed v_r (m/sec)	15
Coefficient of direct cost (Rs/kWh)	4.00
Coefficient of underestimation cost (Rs/kWh)	17.280
Coefficient of overestimation cost (Rs/kWh)	12.280

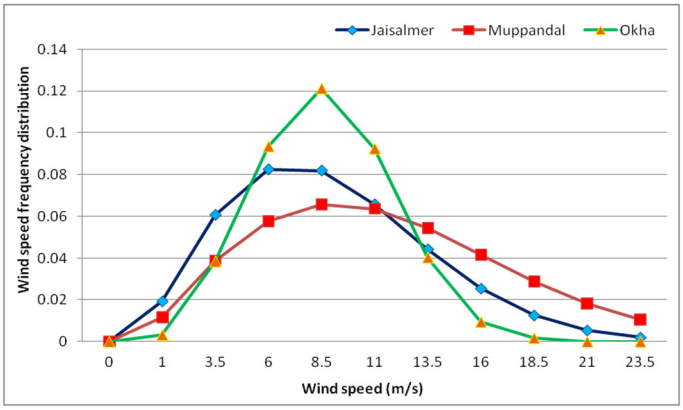

Figure 3. Variation of wind speed frequency distributions with wind speeds of Muppandal, Jaisalmer, & Okha.

Figure 3 represents the variation of wind speed frequency distributions with a range of wind speeds, at 1 PM on the 15th day of June of each year, for Muppandal, Jaisalmer, and Okha. It can be seen that all three places have divergent heights and areas of their wind frequency curves because of their distinct wind distributions. The PDF of wind powers is determined from Eqs (11–13) and available wind powers for different locales are observed from Eq (14). The direct cost, overestimation cost, underestimation cost, and total operating wind power cost for all three wind power systems are evaluated from Eqs (15–18). Depending upon the regional wind distributions for the considered period of specified zones, the available wind powers are observed as 20.869565 MW, 14.3478 MW, and 13.565217 MW for Muppandal, Jaisalmer, and Okha, respectively.

The solar data is examined under the normal distribution of solar irradiance. The PDF of solar radiation is determined with the help of standard deviations and the mean of solar irradiance of three considered places (Figure 4), using Eq (19). The hourly beam solar irradiance incidents on an inclined plane are calculated with the help of Eq (21). The angle of declination of the sun is obtained from Eq (22). The available solar power depends upon solar radiation and the reference temperature of the examined area. Since Jaisalmer has the highest values of both of these variables for the testing

interval, therefore it has the highest available solar power (27.39851 MW), which is succeeded by Muppandal (25.26320660 MW) and Okha (24.02259351 MW). The direct cost, overestimation cost, underestimation cost, and total solar power cost are obtained from Eqs (23–26). Transmission losses of the system are observed from Eqs (27–30). Fuzzy cardinal priority ranking of non-dominating solutions is employed to obtain the best compromise solution (BCS), with the help of Eqs (44–45).

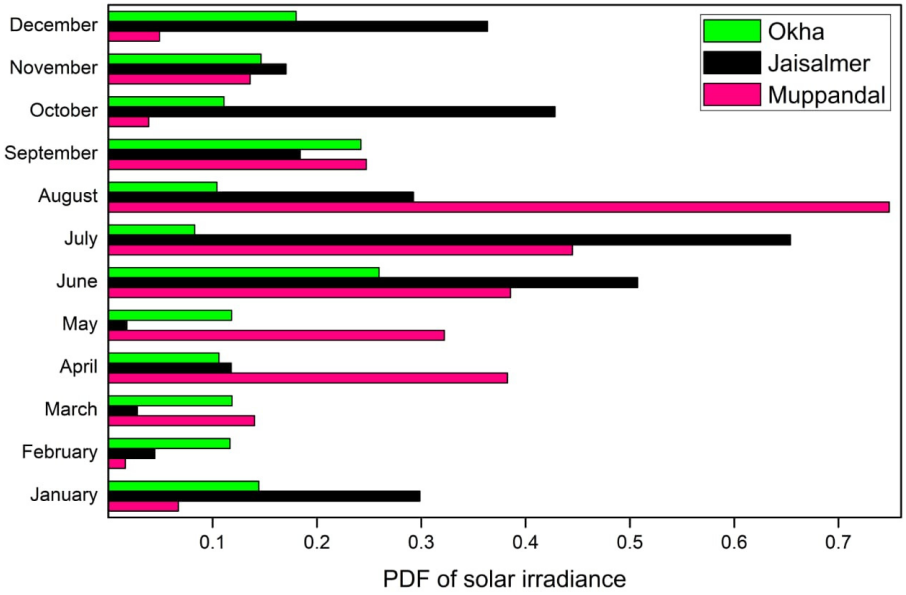

Figure 4. Variation of PDF of solar irradiance of Muppandal, Jaisalmer, & Okha, over the year.

4.2.1. Test system-I (power demand = 250 MW)

This test system is comprised of power scheduling of solar-wind-thermal of three inspected places of India for 250 MW power demand. Since Muppandal has the maximum available wind power for the given spell, therefore it has the maximum scheduled wind power (40.1869 MW). It is found that Muppandal has the highest direct cost of wind power (97654.1700 Rs/h), which is followed by Jaisalmer 68422.3300 Rs/h and Okha (65499.0300 Rs/h). After optimizing the power scheduling problem, the values of fuel cost, NO_x emission, SO_2 emission, CO_2 emission, total operating cost of wind system, total operating cost of solar system, transmission losses, and simulation time for Muppandal, Jaisalmer, and Okha are obtained as 1765.4010 Rs/h, 519.1340 kg/h, 1059.7230 kg/h, 5600.0180 kg/h, 103553.3200 Rs/h, 135482.1000 Rs/h, 3.872521 MW/h & 0.78 sec; 1846.7690 Rs/h, 513.3438 kg/h, 1108.5220 kg/h, 5444.6470 kg/h, 36270.0900 Rs/h, 147552.5000 Rs/h, 4.263066 MW/h & 0.78 sec, and 1906.8030 Rs/h, 514.9072 kg/h, 1144.5360 kg/h, 793.7719 kg/h, 66702.1700 Rs/h, 127596.0000 Rs/h, 4.554507 MW/h & 0.78 sec, respectively, with ACSM. The solution of power scheduling problem of test system-I by using ACSM is tabulated in Table 5.

Table 5. Solution of power scheduling problem of test system-I, by using ACSM.

Output variables			Muppandal	Jaisalmer	Okha
Thermal	Scheduled power (MW)	Unit 1	81.456790	87.801320	89.685880
power		Unit 2	81.599080	85.044940	90.563100
system	Fuel cost (Rs/h)	Unit 1	959.3652	1013.47900	1029.5740
		Unit 2	806.0356	833.2900	877.2296
	Total fuel cost (Rs/h)		1765.4010	1846.7690	1906.8030
	NO_x emission (kg/h)	Unit 1	459.4841	451.4910	449.2212
		Unit 2	59.64996	61.85275	65.6860
	Total NO_x emission (kg/h)		519.1340	513.3438	514.9072
	SO_2 emission (kg/h)	Unit 1	576.1001	608.5461	618.1964
		Unit 2	483.6227	499.9755	526.3396
	Total SO_2 emission (kg/h)		1059.7230	1108.5220	1144.5360
	CO_2 emission (kg/h)	Unit 1	1488.2030	1521.6650	1533.2550
		Unit 2	4111.8150	3922.9820	3640.5310
	Total CO_2 emission (kg/h)		5600.0180	5444.6470	793.7719
Wind	Shape factor-k		2.229	2.86	3.33
power	Scale factor-c (m/s)		12.981	10.099	9.695
system	Scheduled power (MW)	Unit 1	19.991970	13.930720	13.420870
		Unit 2	20.19493	14.22662	13.533470
	Direct cost (Rs/h)	Unit 1	48580.4900	33851.6400	32612.7100
		Unit 2	49073.6800	34570.6900	32886.3200
	Underestimation cost (Rs/h)	Unit 1	11526.6200	8358.1600	3408.3810
		Unit 2	8860.8800	2428.4010	749.6717
	Overestimation cost (Rs/h)	Unit 1	−8191.3680	−5939.7110	−2422.1590
		Unit 2	−6296.9700	−1725.7400	−532.7528
	Operating cost (Rs/h)	Unit 1	51915.7300	36270.0900	33598.9300
		Unit 2	51637.5900	35273.3500	33103.2400
	Total operating cost (Rs/h)		103553.3200	71543.4400	66702.1700
Solar	Scheduled power (MW)	Unit 1	25.455080	27.021360	23.793190
power		Unit 2	25.174760	26.238200	23.558000
system	Direct cost (Rs/h)	Unit 1	68219.6200	72417.2400	63765.7500
		Unit 2	67468.3700	70318.3700	63135.4400
	Underestimation cost (Rs/h)	Unit 1	−1320.1950	4083.7060	793.7719
		Unit 2	608.5282	12563.6500	1607.5670
	Overestimation cost (Rs/h)	Unit 1	938.1940	−2902.0780	−564.0925
		Unit 2	−432.4494	−8928.3350	−1142.4150
	Operating cost (Rs/h)	Unit 1	67837.6200	73598.8700	63995.4300
		Unit 2	67644.4500	73953.6800	63600.5900
	Total operating cost (Rs/h)		135482.1000	147552.5000	127596.000
Total operating cost of RER based power (Rs/h)			239035.4200	219095.9400	194298.170
Transmission losses (MW)			3.872521	4.263066	4.554507
Simulation time (sec)			0.78	0.78	0.78

Figure 5 represents the comparison of load shared by thermal, solar, and wind powers for Muppandal, Jaisalmer, and Okha. Jaisalmer has the highest PDF of solar radiation for the considered time. Therefore, the solar power generated here is about 21% of the total power generated by the coordinated system. Load shared by solar power in Muppandal and Okha is 20% and 19%, respectively.

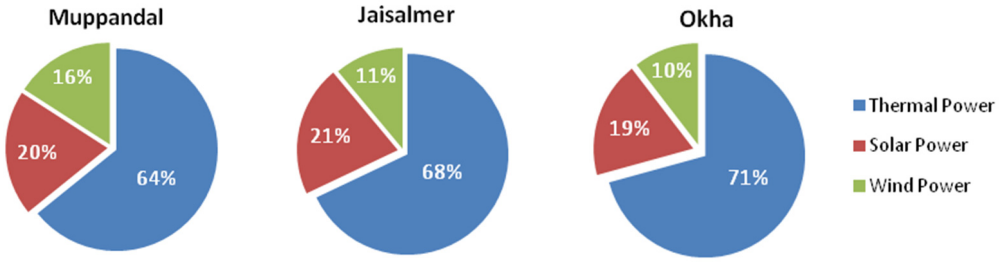

Figure 5. Load shared by thermal, solar, and wind powers in Muppandal, Jaisalmer, & Okha.

Muppandal has the lowest value of shape factor (k = 2.229) and highest value of scale factor (c = 12.981 m/sec). The mean wind speed in Muppandal is 11.50 m/s. Therefore, the generated wind power is about 16% of the total power generated by the system, whereas this value is 11% for Jaisalmer and 10% for Okha. The overall load share of RER-based power is found 36% for Muppandal, 33% for Jaisalmer, and 29% for Okha. Therefore, the thermal power generation is the minimum at Muppandal (64%), for the examined period.

4.2.2. Test system II (power demand = 400)

Test system-II comprehends the same set of six generators as used in test system-I but the power demand is increased from 250 MW to 400 MW. Since the parameters of solar and wind systems are not changed, therefore, the available solar and wind powers are also not changed. Now, the extra load is supplied by the thermal generating system. It is therefore the value of fuel cost, NO_x emission, SO_2 emission, and CO_2 emission also arise. These values are observed for Muppandal, Jaisalmer, and Okha as 3118.4610 Rs/h, 546.6220 kg/h, 1871.3220 kg/h & 4722.1490 kg/h; 3204.7020 Rs/h, 552.6953 kg/h, 1923.0520 kg/h & 4885.2050 kg/h; and 3277.6320 Rs/h, 560.0665 kg/h, 1966.8020 kg/h & 5030.6830 kg/h, respectively. The total operating costs of RER-based power are almost similar to the previous system. These are 237429.1900 Rs/h, 218736.6800 Rs/h, &197487.2300 Rs/h for Muppandal, Jaisalmer, and Okha, respectively. There is a slight change in simulation time this time. It has increased from 0.78 sec to 0.79 sec. The results of test system II using ACSM are tabulated in Table 6.

Table 6. Solution of power scheduling problem of test system II, by using ACSM.

Output variables			Muppandal	Jaisalmer	Okha
Thermal power system	Scheduled Power (MW)	Unit 1	161.02400	166.45350	170.03970
		Unit 2	161.29570	165.66960	170.32660
	Fuel cost (Rs/h)	Unit 1	1645.8460	1693.3100	1724.7040
		Unit 2	1472.6160	1511.3920	1552.9280
	Total fuel cost (Rs/h)		3118.4610	3204.7020	3277.6320
	NO_x emission (kg/h)	Unit 1	398.4640	397.4069	396.9263
		Unit 2	148.1580	155.2884	163.1401
	Total NO_x emission (kg/h)		546.6220	552.6953	560.0665
	SO_2 emission (kg/h)	Unit 1	987.7449	1016.2100	1035.0370
		Unit 2	883.5767	906.8428	931.76480
	Total SO_2 emission (kg/h)		1871.3220	1923.0520	1966.8020
	CO_2 emission (kg/h)	Unit 1	2527.8060	2647.8530	2730.5850
		Unit 2	2194.3430	2237.3520	2300.0980
	Total CO_2 emission (kg/h)		4722.1490	4885.2050	5030.6830
Wind power system	Shape factor-k		2.229	2.86	3.33
	Scale factor-c (m/s)		12.981	10.099	9.695
	Scheduled Power (MW)	Unit 1	20.67054	14.03151	13.34126
		Unit 2	20.56050	14.06176	13.28956
	Direct cost (Rs/h)	Unit 1	50229.4200	34096.5700	32419.2600
		Unit 2	49962.0000	34170.1000	32293.6310
	Underestimation cost (Rs/h)	Unit 1	2614.0010	6338.3090	5288.0540
		Unit 2	4059.3600	5732.1317	6508.7900
	Overestimation cost (Rs/h)	Unit 1	−1857.6350	−4504.3080	−3757.9460
		Unit 2	−2884.7800	−4073.5300	−4625.4580
	Operating cost (Rs/h)	Unit 1	50985.7900	35930.5000	33949.3700
		Unit 2	51136.6000	35828.6800	34176.9610
	Total operating cost (Rs/h)		102122.3900	71759.1800	68126.3310
Solar power system	Scheduled Power (MW)	Unit 1	25.42640	27.49806	24.43054
		Unit 2	24.94910	27.03075	23.97192
	Direct cost (Rs/h)	Unit 1	68142.7700	73694.8000	65473.8400
		Unit 2	66863.5900	72442.4000	64244.7600
	Underestimation cost (Rs/h)	Unit 1	−1122.8950	−1077.8910	−1411.5360
		Unit 2	2161.2340	3982.0750	175.3275
	Overestimation cost (Rs/h)	Unit 1	797.9830	766.0012	1003.1060
		Unit 2	−1535.8770	−2829.8540	−124.5962
	Operating cost (Rs/h)	Unit 1	67817.8500	73382.9100	65065.4100
		Unit 2	67488.9500	73594.6200	64295.4900
	Total operating cost (Rs/h)		135306.8000	146977.500	129360.900
Total operating cost of RER based power (Rs/h)			237429.1900	218736.680	197487.230
Transmission losses (MW)			13.926230	14.74452	15.399560
Simulation time (sec)			0.79	0.79	0.79

5. Comparisons

Table 7. Comparison of results.

Applied Technique	Test System	F_1 (Rs/h)	F_2 (kg/h)			Y_{SQ} (Rs/h)	Y_{wj} (Rs/h)	μ_a^k	Simulation Time (sec)
			NO_x emission	SO_2 emission	CO_2 emission				
MUPPANDAL									
EM	I	1770.6972	540.6914	1062.9021	5616.8181	135888.5460	103863.9800	0.291	4.61
	II	3127.8164	548.2619	1876.9360	4736.3155	135712.7200	102428.7570	0.290	4.67
SM	I	1768.9318	520.1723	1061.8425	5611.2180	135753.0640	103760.4270	0.412	1.42
	II	3124.6979	547.7152	1875.0646	4731.5933	135577.4140	102326.6350	0.411	1.44
SMM	I	1768.0491	519.9127	1061.3126	5608.4180	135685.3230	103708.6500	0.453	1.52
	II	3123.1387	547.4419	1874.1290	4729.2322	135509.7600	102275.5740	0.451	1.52
PSO	I	1767.1664	519.6531	1060.7827	5605.6180	135617.5820	103656.8730	0.472	1.51
	II	3121.5795	547.1686	1873.1933	4726.8711	135442.1070	102224.5120	0.470	1.50
ACSM	I	1765.4010	519.1340	1059.7230	5600.0180	135482.1000	103553.3200	0.592	0.78
	II	3118.4610	546.6220	1871.3220	4722.1490	135306.8000	102122.3900	0.589	0.79
JAISALMER									
EM	I	1852.3093	514.8838	1111.8476	5460.9809	147995.1570	71758.0703	0.292	4.71
	II	3214.3161	554.3533	1928.8211	4899.8606	147418.4330	71974.4575	0.290	4.73
SM	I	1850.4625	514.3705	1110.7390	5455.5362	147847.6050	71686.5269	0.412	1.42
	II	3211.1114	553.8007	1926.8981	4894.9754	147271.4550	71902.6984	0.413	1.43
SMM	I	1849.5392	514.1138	1110.1848	5452.8140	147773.8290	71650.7552	0.453	1.51
	II	3209.5090	553.5243	1925.9366	4892.5328	147197.9660	71866.8188	0.451	1.52
PSO	I	1848.6158	513.8571	1109.6305	5450.0917	147700.0530	71614.9834	0.472	1.51
	II	3207.9067	553.2480	1924.9750	4890.0902	147124.4770	71830.9392	0.471	1.50
ACSM	I	1846.7690	513.3438	1108.5220	5444.6470	147552.5000	71543.4400	0.592	0.78
	II	3204.7020	552.6953	1923.0520	4885.2050	146977.5000	71759.1800	0.590	0.79
OKHA									
EM	I	1912.5234	516.4519	1147.9696	796.1532	127978.7880	66902.2765	0.291	4.68
	II	3287.4649	561.7467	1972.7024	5045.7751	129748.9830	68330.7100	0.289	4.72
SM	I	1910.6166	515.9370	1146.8250	795.3594	127851.1920	66835.5743	0.414	1.42
	II	3284.1873	561.1866	1970.7356	5040.7443	129619.6220	68262.5837	0.411	1.43
SMM	I	1909.6632	515.6796	1146.2528	794.9626	127787.3940	66802.2233	0.453	1.52
	II	3282.5485	560.9066	1969.7522	5038.2290	129554.9410	68228.5205	0.451	1.52
PSO	I	1908.7098	515.4221	1145.6805	794.5657	127723.5960	66768.8722	0.473	1.50
	II	3280.9096	560.6266	1968.7688	5035.7137	129490.2610	68194.4573	0.471	1.50
ACSM	I	1906.8030	514.9072	1144.5360	793.7719	127596.0000	66702.1700	0.592	0.78
	II	3277.6320	560.0665	1966.8020	5030.6830	129360.9000	68126.3310	0.589	0.79

Test system-I & II are also validated with PSO, SMM, SM, & EM, and obtained results are charted in Table 7. It can be seen that ACSM possesses the highest value of Cardinal Priority Ranking and least values of fuel cost & emissions for both the test systems. It takes the least time to

achieve BCS as compared to the other four techniques and also its performance is not affected by using a large number of decision variables.

The box plots in Figure 5 differentiate the functioning of ACSM, PSO, SMM, SM, and EM, for test system-II. The maximum and minimum values of fuel cost using ACSM, PSO, SMM, SM, and EM are 3120.6821 Rs/h, 3123.7210 Rs/h, 3127.3576 Rs/h, 3128.7332 Rs/h, & 3137.3529 Rs/h; and 3117.3257 Rs/h, 3118.7831 Rs/h, 3120.3742 Rs/h, 3120.9759 Rs/h, & 3122.9487 Rs/h, respectively. Also, the difference between first quartile Q_1 and third quartile Q_3 of cost function using ACSM, PSO, SMM, SM, and EM are 0.5532 Rs/h, 1.2460 Rs/h, 2.4606 Rs/h, 3.0599 Rs/h, & 4.1751 Rs/h, respectively. All these factors delineate the superiority of ACSM over other four tested techniques.

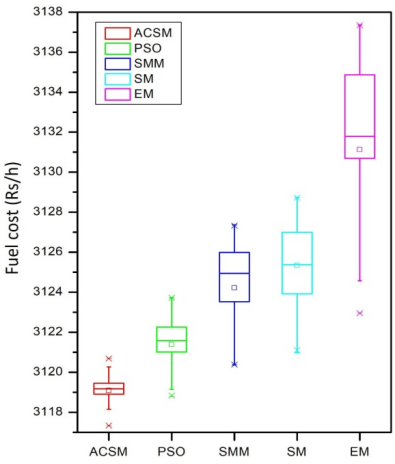

Figure 6. Comparison of fuel costs using ACSM, PSO, SMM, SM, and EM, for test system-II.

6. Conclusions

The integration of large-scale RER is of substantial thrust to electrical energy economizing and limiting emissions. The intensive solar and wind power plant constitutes an auspicious alternative source of RER technology. It also acknowledges the amalgamation of thermal power storage for the accumulation of energy for future utilizations, but RER poses multiple obstacles for power systems because of their changeability, uncertainty, and discontinuity. The employment of RER through prudent scheduling and consigning of power can impart operative pliability into the electrical power system.

In this paper, a multi-objective coordinated solar-wind-thermal power scheduling problem is formulated and optimized for two conflicting economic and environmental objectives. ACSM has been successfully employed in the presented non-linear optimization problem and results are contrasted with some other existing popular population-based techniques. ACSM displays significant competence to runoff from local best solutions because the priority is given to the satisfaction level over the value of the objective function, by applying α-level comparisons. The addition of mutation of the least wanted point and multi-simplexes enhances the exactness of the technique. Therefore, it lowers the probability of missing out on the points around the boundary, during the reduction of the simplex. It is an effective method for constrained optimization because ACSM remains ineffective even when parameters are reshaping. It is a very quick, lethal, and stable technique for constrained optimization problems.

Acknowledgement

I.K. Gujral Punjab Technical University, Kapurthala, India is admiringly acknowledged.

Conflict of interest

The authors reveal that they don't have any conflicts of interest to describe regarding this study.

References

1. Ministry of New and Renewable Energy, Government of India. Annual Report 2018–19. Available from: https://mnre.gov.in/.
2. Liaquat S, Fakhar MS, Kashif SAR, et al. (2021) Application of dynamically search space squeezed modified firefly algorithm to a novel short term economic dispatch of multi-generation systems. *IEEE Access* 9: 1918–1939. https://doi.org/10.1109/ACCESS.2020.3046910
3. Rahimi M, Ardakani FJ, Ardakani AJ (2021) Optimal stochastic scheduling of electrical and thermal renewable and non-renewable resources in virtual power plant. *Int J Elect Power Energy Syst* 127: 106658. https://doi.org/10.1016/j.ijepes.2020.106658
4. Naversen CØ, Helseth A, Li B, et al. (2020) Hydrothermal scheduling in the continuous-time framework. *Electr Power Sys Res* 189: 106787. https://doi.org/10.1016/j.epsr.2020.106787
5. Narang N, Dhillon JS, Kothari DP (2014) Scheduling short-term hydrothermal generation using predator prey optimization technique. *Appl Soft Comp* 21: 298–308. https://doi.org/10.1016/j.asoc.2014.03.029
6. Singh NJ, Dhillon JS, Kothari DP (2018) Multiobjective thermal power load dispatch using adaptive predator-prey optimization. *Appl Soft Comp* 66: 370–383. https://doi.org/10.1016/j.asoc.2018.02.006
7. Mondal S, Bhattacharya A, Dey SHN (2013) Multiobjective economic emission load dispatch solution using gravitational search algorithm and considering wind power penetration. *Int J Elect Power Energy Syst* 44: 282–292. https://doi.org/10.1016/j.ijepes.2012.06.049
8. Ansari MM, Guo C, Shaikh M, et al. (2020) Considering the uncertainty of hydrothermal wind and solar-based DG. *Alex Eng J* 59: 4211–4236. https://doi.org/10.1016/j.aej.2020.07.026
9. Das S, Bhattacharya A, Chakraborty AK (2018) Fixed head short-term hydrothermal scheduling in presence of solar and wind power. *Energy Strat Re* 22: 47–60. https://doi.org/10.1016/j.esr.2018.08.001
10. Dasgupta K, Roy PK, Mukherjee V (2020) Power flow based hydro-thermal-wind scheduling of hybrid power system using sine cosine algorithm. *Electr Power Syst Res* 178: 106018. https://doi.org/10.1016/j.epsr.2019.106018
11. Ji B, Zhang B, Yu SS, et al. (2021) An enhanced borg algorithmic framework for solving the hydrothermal-wind co-scheduling problem. *Energy* 218: 119512. https://doi.org/10.1016/j.energy.2020.119512
12. Reddy SS, Praveen P, Kumari S (2009) Micro genetic algorithm based optimal power dispatch in multimode electricity market. *Int J Recent Trends Eng* 2: 298–302. Available from: https://www.researchgate.net/publication/265432818.

13. Reddy SS (2016) Congestion management using multi-objective grenade explosion method. *WSEAS Transactions power syst* 11: 81–89. Available from: https://www.semanticscholar.org/paper/Congestion-Management-Using-Multi-Objective-Grenade-Reddy/9772b35c435bf21151376567f091b81860066523.
14. Reddy SS (2018) Multi-objective optimization considering cost, emission and loss objectives using PSO and fuzzy approach. *Int J Eng Tech* 7: 1552–1557. https://doi.org 10.14419/ijet.v7i3.11203
15. Salkuti SR (2020) Optimal day-ahead renewable power generation scheduling of hybrid electrical power system. In: Ray P, Biswal M, *Microgrid: Operation, Control, Monitoring and Protection. Lecture Notes in Electrical Engineering* 625: 27–49. https://doi.org/10.1007/978-981-15-1781-5_2
16. Salkuti SR (2020) Multi-objective based economic environmental dispatch with stochastic solar-wind-thermal power system. *Int J Elect Comp Eng* 10: 4543–4551. https://doi.org/10.11591/ijece.v10i5.pp4543-4551
17. Salkuti SR (2021) Multi-objective based optimal network reconfiguration using crow search algorithm. *Int J Adv Comp Sci Appl* 12: 86–95. https://doi.org/10.14569/IJACSA.2021.0120310
18. Zhang X, Xu H, Yu T, et al. (2016) Robust collaborative consensus algorithm for decentralized economic dispatch with a practical communication network. *Elect Power Syst Res* 140: 597–610. https://doi.org/10.1016/j.epsr.2016.05.014
19. Zhang X, Yu T, Yang B, et al. (2016) Virtual generation tribe based robust collaborative consensus algorithm for dynamic generation command dispatch optimization of smart grid. *Energy* 101: 34–51. https://doi.org/10.1016/j.energy.2016.02.009
20. Zhang X, Yu T, Xu Z, et al. (2018) A cyber-physical-social system with parallel learning for distributed energy management of a microgrid. *Energy* 165: 205–221. https://doi.org/10.1016/j.energy.2018.09.069
21. Tan Z, Zhang X, Xie B, et al. (2018) Fast learning optimiser for real-time optimal energy management of a grid-connected microgrid Source. *IET Generation Trans Distrib* 12: 2977–2987. https://doi.org/10.1049/iet-gtd.2017.1983
22. Biswas PP, Suganthan PN, Amaratunga GAJ (2017) Optimal power flow solutions incorporating stochastic wind and solar power. *Energy Conv Manage* 148: 1194–1207. https://doi.org/10.1016/j.enconman.2017.06.071
23. Das S, Bhattacharya A, Chakraborty AK (2018) Solution of short-term hydrothermal scheduling problem using quasi-reflected symbiotic organisms search algorithm considering multi-fuel cost characteristics of thermal generator. *Ara J Sci Eng* 43: 2931–2960. https://doi.org/10.1007/s13369-017-2973-5
24. He Z, Zhou J, Sun N, et al. (2019) Integrated scheduling of hydro, thermal and wind power with spinning reserve. *Energy Procedia* 158: 6302–6308. https://doi.org/10.1016/j.egypro.2019.01.409
25. Kansal V, Dhillon JS (2020) Emended salp swarm algorithm for multiobjective electric power dispatch problem. *Appl Soft Comput* 90: 106172. https://doi.org/10.1016/j.asoc.2020.106172
26. Li J, Lu J, Yao L, et al. (2019) Wind-solar-hydro power optimal scheduling model based on multi-objective dragonfly algorithm. *Energy Procedia* 158: 6217–6224. http://dx.doi.org/10.1016/j.egypro.2019.01.476

27. Panda A, Tripathy M (2016) Solution of wind integrated thermal generation system for environmental optimal power flow using hybrid algorithm. *J Elect Syst Inform Tech* 3: 151–160. https://doi.org/10.1016/j.jesit.2016.01.004
28. Takahama T, Sakai S (2005) Constrained optimization by applying the /spl alpha/ constrained method to the nonlinear simplex method with mutations. *IEEE Tran Evol Comput* 9: 437–450. https://doi.org/10.1109/TEVC.2005.850256
29. Brar YS, Dhillon JS, Kothari DP (2005) Fuzzy satisfying multi-objective generation scheduling based on simplex weightage pattern search. *Int J Elect Power Ener Syst* 27: 518–527. http://dx.doi.org/10.1016/j.ijepes.2005.06.002
30. Kothari DP, Dhillon JS (2011) *Power systems optimization*, 2nd Ed, New Delhi: PHI Learning. Available from: http://www.kopykitab.com/product/7450.
31. Kaur S, Brar YS, Dhillon JS (2020) Solar-thermal power scheduling by inserting α-constrained method to nonlinear simplex method with mutations. *In: 2020 Inter Conference on Smart Grid and Clean Energy Tech (ICSGCE)*, 27–34. http://dx.doi.org/10.1109/ICSGCE49177.2020.9275629
32. Kaur S, Brar YS, Dhillon JS (2020) Multi-objective power scheduling of wind-thermal integrated system by using α-constrained simplex method. *In: 2020 Inter Conference on Smart Grid and Clean Energy Tech (ICSGCE)*, 112–119. https://doi.org/10.1109/ICSGCE49177.2020.9275653
33. Kaur S, Brar YS, Dhillon JS (2021) Optimal scheduling of solar-wind-thermal integrated system using α-constrained simplex method. *Int J Renewable Energy Dev* 10: 47–59. https://doi.org/10.14710/ijred.2021.32245
34. Kaur S, Brar YS, Dhillon JS (2021) Real-time short-term hydro-thermal-wind-solar power scheduling using meta-heuristic optimization technique. *Int J Renewable Energy Dev* 10: 635–651. https://doi.org/10.14710/ijred.2021.35558
35. Reddy SS (2017) Optimal scheduling of wind-thermal power system using clustered adaptive teaching learning based optimization. *Elec Eng* 99: 535–550. https://doi.org/10.1007/s00202-016-0382-5
36. Nagababu G, Baivishi D, Kachhwaha SS, et al. (2015) Evaluation of wind resource in selected locations in Gujarat. *Energy Procedia* 79: 212–219. https://doi.org/10.1016/j.egypro.2015.11.467
37. Singal RK (2010) *Non-conventional energy resources*, 3rd Ed, New Delhi: SK Kataria & Sons. Available from: https://www.skkatariaandsons.com/view_book.aspx?productid=8063.
38. NCERT India. Available from: https://ncert.nic.in/textbook/pdf/iess101.pdf.
39. Muppandal wind farm. Wikipedia the free encyclopedia. Available from: https://en.wikipedia.org/wiki/Muppandal_Wind_ Farm.
40. Sukkiramathi K, Seshaiah CV (2020) Analysis of wind power potential by the three-parameter weibull distribution to install a wind turbine. *Energy Exp Exploit* 38: 158–174. https://doi.org/10.1177%2F0144598719871628

41. Jaisalmer wind park. Wikipedia the free encyclopedia. Available from: https://en.wikipedia.org/wiki/Jaisalmer_Wind_Park.